The dual-function chaperone HycH improves assembly of the formate hydrogenlyase complex

Lindenstrauß, Ute; Skorupa, Philipp; McDowall, Jennifer S.; Sargent, Frank; Pinske, Constanze

Published in:
Biochemical Journal

DOI:
10.1042/BCJ20170431

Publication date:
2017

Licence:
No Licence / Unknown

Document Version
Publisher's PDF, also known as Version of record

Biochemical Journal (2017) **474** 2937–2950
DOI: 10.1042/BCJ20170431

Research Article

The dual-function chaperone HycH improves assembly of the formate hydrogenlyase complex

Ute Lindenstrauß[1], Philipp Skorupa[1], Jennifer S. McDowall[2], Frank Sargent[2] and Constanze Pinske[1]

[1]Martin-Luther University Halle-Wittenberg, Institute of Biology/Microbiology, Kurt-Mothes-Str. 3, 06120 Halle, Germany; [2]School of Life Sciences, Division of Molecular Microbiology, University of Dundee, Dow Street, DD1 5EH Dundee, U.K.

Correspondence: Constanze Pinske (constanze.pinske@mikrobiologie.uni-halle.de)

The assembly of multi-protein complexes requires the concerted synthesis and maturation of its components and subsequently their co-ordinated interaction. The membrane-bound formate hydrogenlyase (FHL) complex is the primary hydrogen-producing enzyme in *Escherichia coli* and is composed of seven subunits mostly encoded within the *hycA-I* operon for [NiFe]-hydrogenase-3 (Hyd-3). The HycH protein is predicted to have an accessory function and is not part of the final structural FHL complex. In this work, a mutant strain devoid of HycH was characterised and found to have significantly reduced FHL activity due to the instability of the electron transfer subunits. HycH was shown to interact specifically with the unprocessed species of HycE, the catalytic hydrogenase subunit of the FHL complex, at different stages during the maturation and assembly of the complex. Variants of HycH were generated with the aim of identifying interacting residues and those that influence activity. The R70/71/K72, the Y79, the E81 and the Y128 variant exchanges interrupt the interaction with HycE without influencing the FHL activity. In contrast, FHL activity, but not the interaction with HycE, was negatively influenced by H37 exchanges with polar residues. Finally, a HycH Y30 variant was unstable. Surprisingly, an overlapping function between HycH with its homologous counterpart HyfJ from the operon encoding [NiFe]-hydrogenase-4 (Hyd-4) was identified and this is the first example of sharing maturation machinery components between Hyd-3 and Hyd-4 complexes. The data presented here show that HycH has a novel dual role as an assembly chaperone for a cytoplasmic [NiFe]-hydrogenase.

Introduction

Mixed acid fermentation enables *Escherichia coli* to grow on glucose in the absence of terminal electron acceptors such as oxygen or nitrate. The main products are ethanol, succinate, lactate, acetate and formate. The latter is further disproportionated to CO_2 and H_2 by the formate hydrogenlyase (FHL) complex during the stationary phase. The FHL complex directly couples the formate-oxidising activity of a formate dehydrogenase (FDH-H) with the proton-reducing activity of [NiFe]-hydrogenase-3 (Hyd-3). This unique composition allows H_2 production without the dependence on electron transfer or energy transduction from other sources [1]. Recently, some challenges in the biochemical characterisation of the FHL complex were overcome by establishing a one-step affinity purification protocol for all seven subunits based on the incorporation of an internal His-tag into the Hyd-3 large subunit, HycE [2]. However, the innate instability of the complex necessitates an improved understanding of the early assembly steps and a putative modification of factors aiding protein stability could make the FHL complex a useful target for *in vitro* H_2 production.

After the genetic locus of the Hyd-3 coding *hycA-I* operon was identified in 1990 [3], a systematic approach identified HycA as having a regulatory function, the *hycB*, *hycF* and *hycG* genes as encoding electron transport proteins and *hycC* and *hycD* as coding for integral membrane subunits. The *hycE* gene was found to encode the catalytic hydrogenase subunit [4]. In that initial study, the apparent

Received: 31 May 2017
Revised: 11 July 2017
Accepted: 17 July 2017

Accepted Manuscript online: 18 July 2017
Version of Record published: 11 August 2017

PORTLAND PRESS

Biochemical Journal (2017) **474** 2937–2950
DOI: 10.1042/BCJ20170431

terminal gene of the operon was *hycH* and, due to the phenotype of the accumulated, inactive large subunit, was considered to be the potential protease specific for HycE processing [4]. However, the introduced *hycH* mutation affected expression of a downstream gene, which was later termed *hycI*. The lack of HycI proved to be responsible for the phenotype of the original mutant [5]. Recently, isolation of affinity-tagged HycE from a genetic background devoid of HycG identified a potential HycE–HycH and HycE–HypC complex [6] although HycH and HypC are not part of the final structural FHL complex [2,4]. It is predicted that in the soluble domain of the FHL complex, HycE interacts directly with its small subunit HycG and the electron transfer subunit HycF, while the FDH-H (FdhF) and its small subunit HycB interact indirectly via HycF [4,7]. The interaction of unprocessed HycE with HypC was established earlier [8,9]. This finding suggested a function for HycH during subunit maturation.

The *fdhF* gene, encoding the FDH-H component of the FHL complex, is not part of the *hycA-I* operon [7].

The genes of a second putative FHL complex have been identified in *E. coli*, encoded by the *hyf* operon [10]. This predicted complex includes the Hyd-4 enzyme, which could form a homologous protein complex to Hyd-3 within an FHL-2 [10]. However, H_2 production by this putative complex has yet to be unambiguously demonstrated and little is known about specific maturation requirements of this complex. The *hyf* operon is not transcribed at a significant level under the conditions where FHL is active [11,12]. Genetic analysis suggests that the *hyf* operon encodes 12 proteins, but no gene for a specific endoprotease equivalent to HycI is present. Rather, five membrane subunits and a transport protein (FocB) with similarity to the formate transporter FocA are encoded by genes within the operon [10]. The predicted hydrogenase protein HyfG amino acid sequence is ~70% identical with the large subunit HycE. The *hyf* operon also encodes a HycH homologue named HyfJ that shares 45% overall amino acid sequence identity with HycH. Clearly, HycH-like accessory proteins have been evolutionarily conserved in FHL-like gene clusters; however, they remain poorly understood in terms of their biochemical activity or physiological role.

All [NiFe]-hydrogenases share the Ni-Fe$(CN)_2CO$ cofactor, which has the diatomic ligands CN^- and CO attached to the Fe-atom. The Hyp proteins are required for cofactor synthesis and once assembled, their delivery to the large subunit HycE is directed by HypC. In a final step, nickel, transported into the cell by the NikABC transporter, is inserted by HypAB to complete active site synthesis. Mutations in genes of nickel metabolism result in the absence of Hyd activity due to the lack of Ni^{2+} availability [13]. Finally, the cofactor is enclosed within the HycE subunit after a protein-specific endoproteolytic cleavage of the HycE polypeptide by HycI, which cleaves off a C-terminal peptide [5]. The resulting smaller HycE protein species can then interact with its cognate small subunits. How these latter processes are controlled is not understood. Therefore, in the present study, we perform a genetic and biochemical characterisation of HycH and demonstrate a role in FHL complex assembly. The data presented here show, for the first time, a protein interaction of a hydrogenase large subunit with its chaperone before complex assembly. It adds to our knowledge of hydrogenase assembly and will provide the basis for improving the stability of these protein complexes for biotechnological applications in biohydrogen production.

Experimental procedures

Strain construction

Strains and plasmids used in the present study are listed in Supplementary Table S2. MGe1dH was constructed by introducing a markerless deletion of *hycH* in MG059e1 [14]. For in-frame deletion of *hycH*, ~500 bp of DNA upstream of the gene, including the first four codons for *hycH*, was amplified by PCR using MG059e1 as a template and cloned as an EcoRI–BamHI fragment into pBluescript. Subsequently, ~500 bp of DNA downstream of the gene, to be deleted including the last 10 codons of *hycH*, was amplified by PCR using MG059e1 as a template and cloned as a BamHI–XbaI fragment into the pBluescript clone containing the cognate upstream DNA fragment. The deletion allele was subsequently excised from pBluescript by digestion with XbaI and KpnI and cloned into similarly digested pMAK705. The deletion allele was then recombined onto the chromosome of strain MG059e1, according to the method of Hamilton et al. [14] to give strain MGe1dH ($_{His}$*hycE*, Δ*hycH*).

The deletions of *hyfG* and *hyfJ* were moved from JW2472 (Δ*hyfG*) and JW2475 (Δ*hyfJ*) from the Keio collection by phage transduction onto MG059e1 and MGe1dH [15,16]. Strain CPH001 was constructed using MC4100 (DE3) as a recipient for the Δ*hycAI*::*kan* allele from CP971 and subsequently removing the resistance cassette using pCP20 [17,18]. The strain was further modified with a Δ*nikC* deletion using a P1*vir* lysate from

Biochemical Journal (2017) **474** 2937–2950
DOI: 10.1042/BCJ20170431

Δ*nikC*::*kan* strain JW3443 from the Keio collection [15] resulting in strain CPH002. Strain CPH003 was constructed using CPH001 and introducing the Δ*hypC* deletion from DHP-C after the 500 bp up- and downstream regions were cloned onto pMAK705 [14,19].

Plasmid constructions

General information about the plasmids can be found in the vector table (Supplementary Table S2). The plasmid pHycEHI was cloned using MG059e1 chromosomal DNA as a template and the oligonucleotides hycE_FW_NcoI and hycE_RW_EcoRI (Supplementary Table S3). The PCR product and pACYC-DuetI were digested with NcoI and EcoRI before being ligated. The *hycH* and *hycI* genes were cloned together into the second multicloning site using the oligonucleotides hycH_NdeI_FW and hycI_KpnI_RW and digestion of PCR fragments and vector with NdeI and KpnI before ligation. Subsequently, the coding sequence of an *N*-terminal StrepII-tag was introduced with the NEBase changer method using the oligonucleotides Strep_hycH_FW and Strep_hycH_RW according to the NEB instructions. The vector was further modified by the deletion of *hycI* via inverse PCR using the oligonucleotides hycI_FW_PvuI and hycI_RW_PvuI, PvuI digestion and subsequent ligation resulting in pHycEH. Alternatively, plasmid pHycEstopHI was obtained by introducing a stop codon at position 551 where the cleavage site for HycI would be (amino acid position 538 in wild-type HycE) using the oligonucleotides HycE_stop_FW and HycE_stop_RW, according to the Stratagene method.

Cloning of pHycG was done by amplifying the *hycG* gene with oligonucleotides hycG_FW_SphI and hycG_RW_BamHI, digesting both pQE70 and the PCR product with SphI and BamHI before ligating.

The *hyfJ* gene was cloned as a NdeI/NdeI fragment containing the StrepII-tag coding sequence in the forward oligonucleotide into pACYC-DuetI and the pACYC-DuetI-containing *hycE*.

Cloning of pHycBFG was done by amplification of the pQE70 vector with pQE_FW and pQE_RW oligonucleotides, the *hycB* gene with hycB_FW and hycB_RW oligonucleotides, and *hycFG* genes together with hycFG_FW and hycFG_RW oligonucleotides. All PCR fragments were assembled with the NEBuilder protocol according to the manufacturer's instructions (New England Biolab). The oligonucleotides were designed to introduce a new ribosome-binding site upstream of *hycF* and using the T5 promoter and ribosome-binding site from the pQE70 vector for *hycB*.

The plasmid pHycEHI was used as a template to introduce the listed site-directed mutations in *hycH* by the NEBase changer method according to the manufacturer's instructions (New England Biolab) and using the oligonucleotides listed in Supplementary Table S3.

Reverse transcription PCR

RNA was isolated from strains in exponential growth phase using the SV Total RNA Isolation System according to the manufacturer's instructions (Promega, U.S.A.). An extra DNase digest was performed using RQ1 RNase-Free DNase (Promega, U.S.A.). The reverse transcription PCR (RT–PCR) to generate cDNA was performed using M-MLV Reverse Transcriptase RNase H− and random hexamer primers according to the manufacturer's instructions (Promega, U.S.A.). The presence of transcripts was tested with gene-specific oligonucleotides listed in Supplementary Table S3.

Growth conditions

Strains were routinely grown on LB agar plates or in LB liquid cultures at 37°C. For assessing FHL activity or content, strains were grown as standing liquid cultures in closed tubes and in TGYEP medium which contained 1% (w/v) tryptone, 0.5% (w/v) yeast extract, 0.1 M potassium phosphate buffer (pH 6.5) and 0.8% (w/v) glucose [20]. When required, chloramphenicol was added to a final concentration of 15 μg ml^{-1}. For protein purifications, the strains were grown anaerobically in TB medium [21] containing 0.4% glucose or TGYEP medium until they reached an optical density of 0.3–0.4 when they were induced with 150 μM IPTG and left at 25°C for another 2–2.5 h before harvesting. The M9-minimal medium used contained 1× M9 salts, 2 mM $MgSO_4$, 0.1 mM $CaCl_2$, 3 μM thiamine hydrochloride, trace element solution SL-A, 0.2% casamino acids and 0.8% (w/v) glucose [21,22].

Protein purifications

Cells were lysed with sonication and, in the MC4100 backgrounds, PMSF was added to prevent protein degradation to a final concentration of 1 mM. The purification of HycE or HyfG was according to ref. [2], except that the DDM detergent was omitted from buffers A and B. Elution was performed as a step gradient with 300 mM

PORTLAND PRESS
Biochemical Journal (2017) 474 2937–2950
DOI: 10.1042/BCJ20170431

imidazole in buffer A and when protein was precipitated, TCA was added to a final concentration of 20% (w/v). For HycH and HyfJ purifications, Streptactin material was used according to the manufacturer's instructions (IBA Lifesciences, Germany).

Polyacrylamide gel electrophoresis and immunoblotting

Generally, Western blot analysis was performed using aliquots of 50 μg of protein derived from cell-free crude extracts, unless stated otherwise. Polypeptides were separated by SDS–polyacrylamide gel electrophoresis (SDS–PAGE) in 12.5% (w/v acrylamide) gels [23]. Transfer of the polypeptide from the gels to nitrocellulose membranes was done as described in ref. [24]. Antibodies raised against HycG (1 : 3000; [4]), Strep-tag HRP conjugate (1 : 10 000; IBA Technologies) and monoclonal anti-His antibody (1 : 10 000; Abcam) were used. A secondary antibody conjugated to horseradish peroxidase was obtained from Bio-Rad. Visualisation was done by the enhanced chemiluminescent reaction (Stratagene).

Enzymatic assays

The FHL activity was assessed using a Clark-type electrode (Oxytherm, Hansatech Instruments, U.K.) in combination with an Oxy/Ecu at −0.7 V (oxygen electrode conditioning unit; Hansatech Instruments, U.K.). A 50–100 μl suspension of cells was introduced into the electrode chamber filled with 2 ml of N_2-saturated MOPS buffer at pH 7.0. The reaction was started by the addition of formate to a final concentration of 15 mM and the slope was recorded. The amount of hydrogen was calculated based on a calibration with H_2 saturated buffer as described before [25].

H_2-dependent reduction in benzyl viologen (BV) was assayed by monitoring the reduction in BV at 600 nm as described in ref. [26].

The H_2 content of the 10 ml gas phase of an overnight culture was measured by sampling 200 or 500 μl in a GC-2010 or GC-2015, respectively. Either system was equipped with a packed column (Molsieve 5A or Shin Carbon Micropacked column ST80/100). The carrier gas was N_2 with a flow rate of 13.9 ml min^{-1}, the injector was kept at 140°C, the column at 110°C and the TCD detector at 150°C and 40 mA.

The determination of protein concentration was done as described in ref. [27].

Results

A *hycH* deletion reduces FHL activity and stability

The availability of both in-frame knockout strains from the *E. coli* Keio collection and analysis of markerless deletions in *hycH* [14,15] showed that the strain still produced H_2 from the FHL complex, which establishes that these strains have a different phenotype to the previously described Δ*hycH* strain [4]. Initially, total hydrogenase activity was assayed in crude extracts as H_2-dependent reduction of BV after 12 h growth of cells. Under these conditions, the activity of the Hyd-3 component of the FHL complex contributes 98% of the hydrogen-dependent BV reduction activity as can be seen when comparing the MG1655 parental strain with that of CP971 (Δ*hycAI*) (Table 1) and which has been established previously [28]. Deletion of *hycH* caused a reduction in the activity of the FHL complex by ∼87–92% compared with the activity of the parental strain, indicating that residual activity of FHL can be detected. Complementation of JW2688KO with *hycH* or *hycH* in combination with *hycE* and *hycI* restored the activity to 110 and 84%, respectively (Table 1).

The headspace of overnight cultures was also assayed for glucose conversion into H_2 by FHL. It showed that a residual 30% (JW2688KO) to 40% (MGe1dH) H_2 was produced by the *hycH* knockout strains. The experiment was also conducted in M9-minimal medium omitting nickel, iron or zinc, which revealed that without nickel or iron, the accumulation of H_2 was further reduced to 20% of the parental level (Supplementary Table S1).

The chromosomal His-tag on the Hyd-3 large subunit HycE allows the purification of the entire FHL complex after solubilisation of the total protein and application to an affinity column [2]. The same purification strategy can be used in combination with genetic modifications on the chromosome, like the *hycH* deletion in strain MGe1dH. The small-scale purification of an exponentially growing culture resulted in the elution of similar proteins based on the protein pattern after SDS–PAGE. Moreover, the amount of protein eluted after purification from both strains was comparable (Figure 1A). The protein composition of the Δ*hycH* (MGe1dH) sample changed notably compared with MG059e1 when the purification was performed after 16 h of growth

Biochemical Journal (2017) **474** 2937–2950
DOI: 10.1042/BCJ20170431

Table 1 H_2 content and total hydrogenase activity measurement

Strain (+plasmid)	Relevant genotype	H_2 produced (μmol H_2 ml^{-1} $OD^{-1}_{600\ nm}$)[1]	Hydrogenase-specific activity (μmol H_2 oxidised min^{-1} mg $protein^{-1}$)[2]
MG1655	Parental	10.3 ± 4.4	4.74 ± 0.97
MG059e1	Internal His on HycE ($_{His}$HycE)	11.1 ± 0.3	n.d.
CP971	Δ*hycAI*	<0.01	0.09 ± 0.01
MGe1dH	$_{His}$HycE Δ*hycH*	4.5 ± 0.2	0.36 ± 0.18
JW2688KO	Δ*hycH*	3.2 ± 0.1	0.60 ± 0.08
JW2688KO + pHycH	Δ*hycH* + *hycH*	9.5 ± 0.8	5.25 ± 0.46
JW2688KO + pHycEHI	Δ*hycH* + *hycEHI*	12.0 ± 3.1	3.99 ± 0.12
MGe1dH + pHycEHI	$_{His}$HycE Δ*hycH* + *hycEHI*	9.0 ± 0.4	n.d.
CPH004	$_{His}$HycE Δ*hyfG*	12.2 ± 1.3	n.d.
CPH005	$_{His}$HycE Δ*hyfJ*	10.6 ± 3.8	n.d.
CPH006	$_{His}$HycE Δ*hycH* Δ*hyfG*	10.0 ± 4.5	n.d.
CPH007	$_{His}$HycE Δ*hycH* Δ*hyfJ*	2.0 ± 0.4	0.30 ± 0.04
JW2688KO + pHyfJ	Δ*hycH* + *hyfJ*	14.9 ± 3.8	4.00 ± 0.66
JW2688KO + pHycE-HyfJ	Δ*hycH* + *hyfJ* + *hycE*	11.8 ± 5.1	1.82 ± 0.18
CPH007 + pHycH	$_{His}$HycE Δ*hycH* Δ*hyfJ* + *hycH*	8.7 ± 0.7	4.77 ± 0.25
CPH007 + pHycEHI	$_{His}$HycE Δ*hycH* Δ*hyfJ* + *hycEHI*	6.4 ± 1.0	3.86 ± 0.24
CPH007 + pHyfJ	$_{His}$HycE Δ*hycH* Δ*hyfJ* + *hyfJ*	11.1 ± 4.4	4.13 ± 0.31
CPH007 + pHycE-HyfJ	$_{His}$HycE Δ*hycH* Δ*hyfJ* + *hyfJ* + *hycE*	11.3 ± 2.8	2.01 ± 0.23

All measurements were done in biological triplicates and values are given as average with their respective standard deviations. Abbreviations: n.d., not determined.
[1]Cells were grown anaerobically in 5 ml of TGYEP (pH 6.5) with a headspace of 10 ml. A volume of 200–500 μl of headspace was sampled for H_2 concentration and the amount of H_2 was calculated based on a calibration curve.
[2]Cells were grown anaerobically in TGYEP and total hydrogenase activity was determined in crude extracts as H_2-dependent BV reduction.

and almost no electron transfer subunits (HycG, HycF and HycB) and FDH-H (FdhF) was attached to HycE in the Δ*hycH* strain (Figure 1B).

To investigate FHL stability at different time points, the small subunit HycG was chosen as an indicator protein, because HycG is readily degraded when it is not attached to the large subunit HycE. Cells were sampled at different time points after inoculation of the culture and HycG was analysed by Western blotting. The comparison showed that HycG was barely detectable after 4 h in MGe1dH (Δ*hycH*), while in the MG059e1 parental strain HycG was detected at all time points up to 23 h (Figure 1C). The HycG protein re-appears in the Δ*hycH* strain at 23 h, which shows that a mechanism for FHL assembly exists that is independent of HycH. Samples were also analysed for specific FHL activity on the electrode using formate as an electron donor. The results showed that strain MGe1dH had the same activity maximum after 6 h of growth but had consistently 75% lower activity than the MG059e1 strain (Figure 1D).

Cross-talk of *hyc* and *hyf* gene products

Initially, RT–PCR was conducted to show that the *hyfJ* gene is transcribed in the MG059e1 and MC4100 backgrounds under the conditions where the cells were grown (Figure 2A). PCR products for *hyfJ*, *hycB* and *hycH* genes were detectable using cDNA as a template. No PCR product was detectable in the RNA and water controls, showing that no contamination with DNA was present. As expected from the previous observation that the *hyf* operon gene products do not contribute to H_2 production in *E. coli* [29], introducing deletions of *hyfG* (the predicted large subunit of Hyd-4, strain CPH004) and *hyfJ* (the HycH homologue for Hyd-4, strain CPH005) had no influence on H_2 production in the MG059e1 parental background. Nevertheless, the influence of the *hyfG* and *hyfJ* deletions on the residual FHL activity was investigated by combining these mutations in

Biochemical Journal (2017) **474** 2937–2950
DOI: 10.1042/BCJ20170431

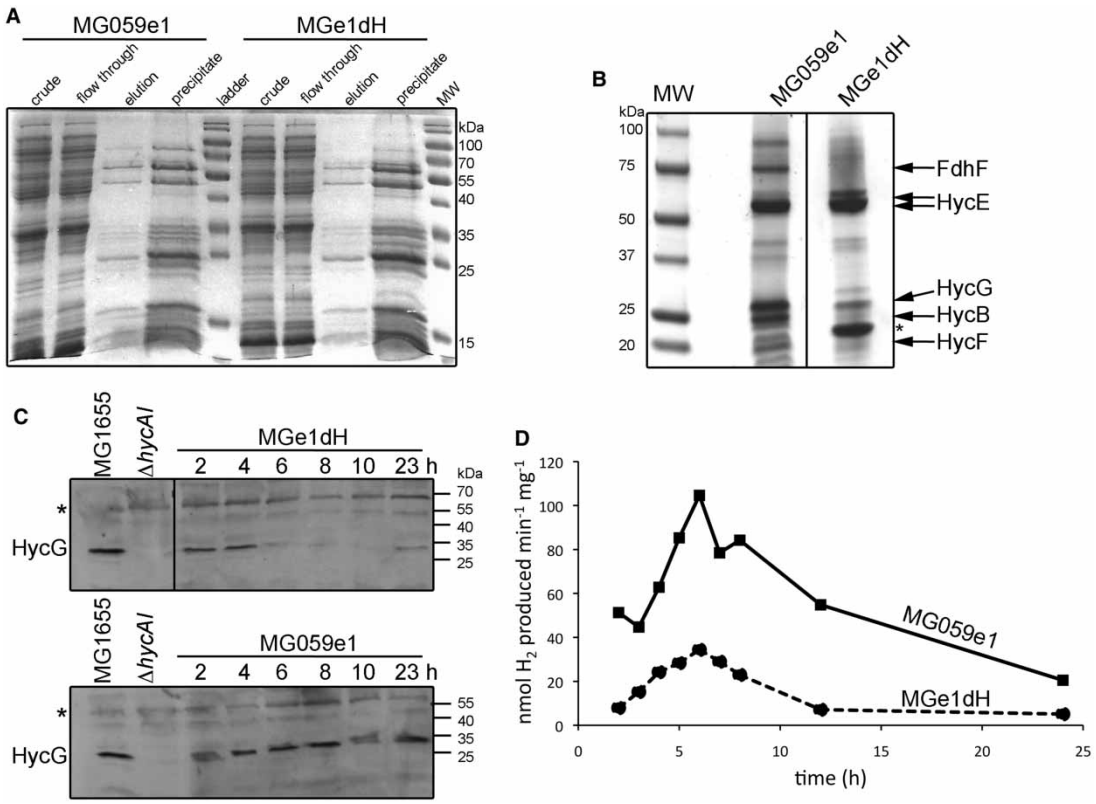

Figure 1. Phenotype of a Δ*hycH* strain.

(**A**) The strains MG059e1 and MGe1dH (Δ*hycH*) were grown anaerobically in TGYEP (pH 6.5) for 6 h and the solubilised total protein was applied to cobalt affinity chromatography (for details, see the Experimental procedures section). The fractions are after solubilisation (crude), unbound protein (flow through), elution fraction with 300 mM imidazole (elution) and the same fraction after TCA precipitation (precipitate). A volume of 4–10 μl was applied to a 12.5% (w/v acrylamide) SDS–PAGE and stained with Coomassie. (**B**) The elution fractions after 16 h growth on a 10% (w/v acrylamide) SDS–PAGE. The asterisk (*) indicates a DNA-binding transcription regulator that co-purified with HycE and was identified by mass spectrometry. (**C**) Crude extracts from strain MG1655, CP971 (Δ*hycAI*), MG059e1 and MGe1dH that were grown anaerobically in TGYEP (pH 6.5) were harvested either after 6 h or as stated and subjected to a 12.5% (w/v acrylamide) SDS–PAGE, separated, transferred to nitrocellulose and challenged with anti-HycG antibodies (1 : 3000). The asterisk indicates a cross-reacting polypeptide that serves as an internal loading control. Molecular weight markers (MW) are included and relative molecular masses indicated. (**D**) Analysis of formate-dependent H_2 production in cells on an electrode, as described in the Experimental procedures section. The squares represent MG059e1 and the circles/dashed line strain MGe1dH.

the Δ*hycH* background resulting in strains CPH006 and CPH007, respectively. Surprisingly, the *hyfJ* deletion reduced H_2 content further to a residual 18% in the Δ*hycH* background, but the *hyfG* deletion reversed the effect of the *hycH* deletion and restored H_2 production to 90% of the level measured in wild-type cultures.

Complementation of the Δ*hycH* strain JW2688KO with *hyfJ* increased H_2 production above wild-type levels (134%), while in the presence of extra copies of *hycE*, the H_2 amount was similar to parental levels (106%). The same observation is reflected in the total hydrogenase activities, which are restored to wild-type levels in the presence of *hyfJ*, but reach only 38% (1.82 U mg^{-1}) when additional copies of *hycE* are simultaneously present in the Δ*hycH* strain JW2688KO.

The *hycH hyfJ* double null mutant CPH007 could be complemented to parental levels of H_2 production by either *hyfJ* or *hyfJ* in combination with *hycE*, but reached only 78 or 58% of the H_2 production when a plasmid with *hycH* or *hycH*, *hycE* and *hycI* was complemented *in trans*, respectively. That total hydrogenase activity is reduced in the presence of extra copies of *hycE* could also be observed in the double mutant CPH007 with plasmids pHycEHI and pHycE-HyfJ (Table 1).

Biochemical Journal (2017) **474** 2937–2950
DOI: 10.1042/BCJ20170431

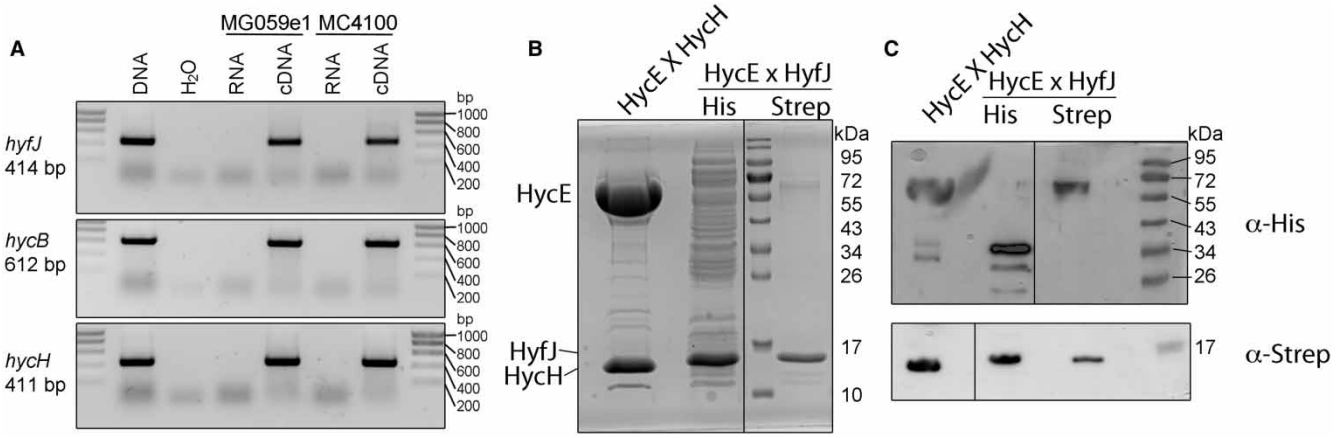

Figure 2. Transcription of *hyfJ* and HyfJ interaction with HycE.

(**A**) A 1% (w/v) agarose gel shows the PCR products *hyfJ* (top), *hycB* (middle) and *hycH* (bottom) from DNA template (DNA), water (H_2O), RNA or cDNA template from the strains MG059e1 or MC4100, as indicated. The sizes are according to SmartLadder (Eurogentec). (**B**) The 12.5% (w/v acrylamide) PAGE shows the HycE and HycH complex as reference and the eluted proteins of BL21(DE3) carrying pHycE-HyfJ after cobalt (His) or Streptactin (Strep) purification. (**C**) The same proteins as in **B** were transferred to nitrocellulose and challenged either with antibodies raised against His8 (top) or with Strep–HRP conjugate (bottom). The migration of HycE, HycH and HyfJ is indicated to the left and the molecular mass is indicated to the right (PageRuler prestained, Thermo Fisher).

All mutant strains showed comparable activities of Hyd-1 and Hyd-2 after native PAGE activity staining (Supplementary Figure S1), indicating that these mutations affected only the activity of the FHL complex.

In accordance with the complementation data are small-scale purifications that show an interaction of HycE and HyfJ by purifying either His-tagged HycE with a cobalt column or Strep-tagged HyfJ with a Streptactin

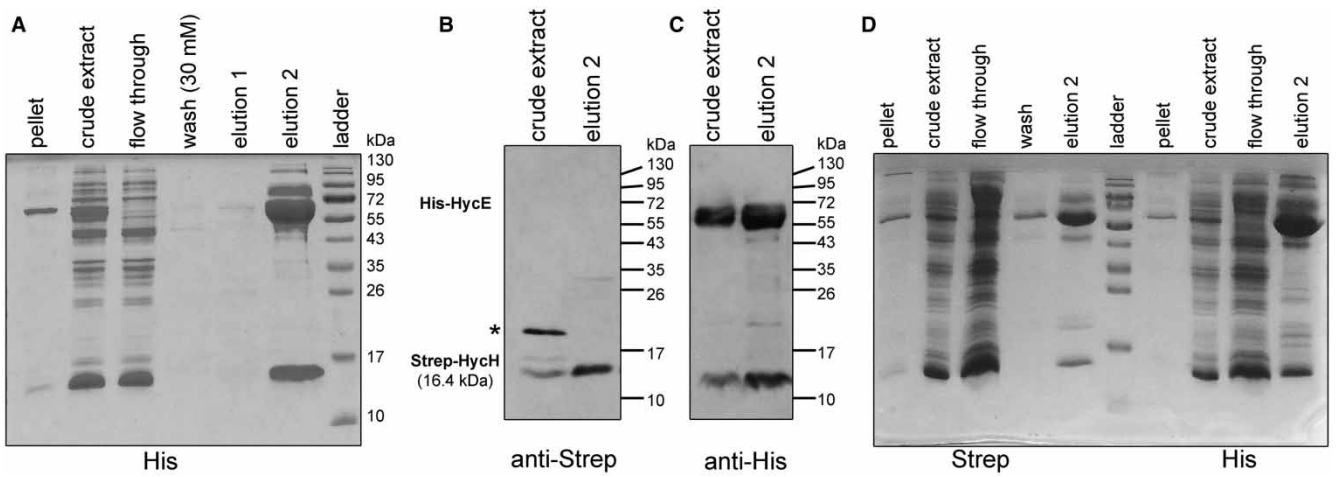

Figure 3. Purification of the HycE and HycH proteins as a complex.

(**A**) The extract from BL21(DE3) carrying pHycEHI was applied to a 1 ml cobalt column and eluted with 300 mM imidazol. The 12.5% (w/v acrylamide) PAGE shows the pellet after gaining the crude extracts, the crude extracts, the flow through of unbound protein, wash fraction with 30 mM imidazol and elution fractions 1 and 2 (300 μl and 1 ml, respectively) with 300 mM imidazol. (**B**) The crude extracts and elution fraction 2 were challenged with a Strep-tag–HRP conjugate that shows a cross-reaction with BCCP in crude extracts and is indicated with an asterisk. (**C**) The same fractions were also analysed for His-tag epitopes. (**D**) A purification with a 1 ml Streptactin (5 lanes on the left) and a 1 ml cobalt column (4 lanes on the right) was performed from pHycEHI expressed in a MC4100(DE3) Δ*hycAI* background (CPH001). Molecular weight markers (MW) are included and relative molecular masses indicated. The migration pattern of the molecular mass standard (ladder, PageRuler prestained, Thermo Fisher) is shown in the middle of panel **D** (and on the right of panels **A**–**C**).

Biochemical Journal (2017) **474** 2937–2950
DOI: 10.1042/BCJ20170431

column from the same extracts (Figure 2B). Although the HycE protein appears degraded after the His-purification which might be due to the high imidazole concentration in the elution buffer, the HyfJ protein co-purified and in reverse the HyfJ protein purification via the Streptactin column co-eluted the HycE protein. The HycE protein is not degraded after Strep purification due to the milder elution conditions. The identities of both proteins and the corresponding control proteins from the HycE × HycH interaction were verified by blotting against the fused polypeptide tags (Figure 2C).

HycH interacts with pre-HycE

Based on the observation that HycH can be co-localised with the Hyd-3 large subunit after the deletion of the small subunit HycG [6], we wished to analyse this interaction in more detail. For this purpose, we used a strain that carried a deletion of the *hyc* operon but encoded the DE3 prophage with the T7 polymerase (CPH001), allowing controlled expression of plasmid-based *hycH*. Alternatively, BL21(DE3) was used as it was previously shown not to have any endogenous FHL activity [18]. The plasmid pHycEHI was introduced in both strains, and after anaerobic growth and induction with IPTG, crude extracts were prepared and applied to either a cobalt column (Figure 3A,D) or a Streptactin column (Figure 3D). In both cases, it was possible to elute two proteins with molecular masses of 67 kDa corresponding to His-tagged HycE ($_{His}$HycE) and 16 kDa corresponding to N-terminally StrepII-tagged HycH ($_{Strep}$HycH). To verify the identity of the proteins, the elution fractions and crude extracts were subjected to Western blot analysis using anti-His antibodies and an anti-Strep–HRP conjugate, and the sizes of the polypeptides identified on the blots corresponded to those of the expected proteins (Figure 3B,C).

The HycE protein undergoes a maturation process before it can interact with the electron transfer subunits [7]. These steps are summarised in Figure 4A and can be broken down into cofactor delivery, nickel insertion, proteolytic processing and interaction with the remainder of the FHL subunits. To dissect the HycE × HycH interaction during these steps, the established purification strategy was modified by introducing the *hypC* deletion in CPH001, which resulted in strain CPH003. HypC delivers the $Fe(CN)_2CO$ moiety of the cofactor to the precursor of HycE and its absence results in an apo-protein lacking any metal cofactor [8]. The resulting purification of either $_{Strep}$HycH or $_{His}$HycE from this strain revealed the concomitant purification of the respective other protein (Figure 4B).

The next step on the maturation pathway is the delivery of nickel in the HycE protein already loaded with the $Fe(CN)_2CO$ cofactor. To test whether nickel delivery influenced the HycH–HycE interaction, nickel transport into the cell was interrupted by introducing a *nikC* deletion into CPH001, resulting in strain CPH002; this mutation results in a nickel-free precursor of HycE [9]. The anticipated hydrogenase-negative phenotype caused by the deletion of *nikC* was verified by the analysis of the H_2-oxidising hydrogenase activity of Hyd-1 in native PAGE [30]. The results showed that Hyd-1 activity was restored to the mutant only after the addition of 500 μM nickel to the growth medium (Supplementary Figure S2). Protein purification of $_{His}$HycE and $_{Strep}$HycH from pHycEHI in this strain background showed a strong interaction of both proteins (Figure 4C).

[NiFe]-cofactor insertion is finalised by an endoproteolytic cleavage event catalysed by the HycE-specific protease HycI. Purification of $_{Strep}$HycH from a strain carrying pHycEH (a vector lacking *hycI*) revealed that HycE was associated with HycH, but it had a slower mobility in the gel (Figure 4D) compared with when it is purified from a strain carrying the pHycEHI plasmid. Purified HycE associated with HycH from the latter strain appears to migrate as a double band, indicating a mixture of processed and unprocessed HycE species attached to HycH (Figure 4D). Therefore, to clarify whether processed HycE can interact with HycH, a genetically modified *hycE* gene was generated with a stop codon introduced at codon 538 (based on the nomenclature of the untagged protein) delivering a protein equivalent to the processed HycE species. This protein mimics the fold of the mature form, but without the necessity of cofactor insertion. This 'genetically processed' variant of HycE no longer co-purified with $_{Strep}$HycH (Figure 4E). Moreover, after purification by the cobalt affinity chromatograph, the HycE variant underwent rapid degradation (Figure 4E) with several bands showing signals after blotting against the His-tag (data not shown).

It is assumed that processed HycE is primed for interaction with HycG. To examine whether an interaction between the two proteins could be determined, the pHycEHI plasmid was co-transformed with pHycG in strain CPH001. The pHycG plasmid is fully functional in complementing FHL activity of a Δ*hycG* strain for H_2 production (data not shown). HycG did not associate with HycE and remained in the insoluble fraction after expression (Figure 4F). HycG also did not co-purify with $_{Strep}$HycH, nor did it influence the interaction between HycH and HycE (Figure 4F).

Biochemical Journal (2017) **474** 2937–2950
DOI: 10.1042/BCJ20170431

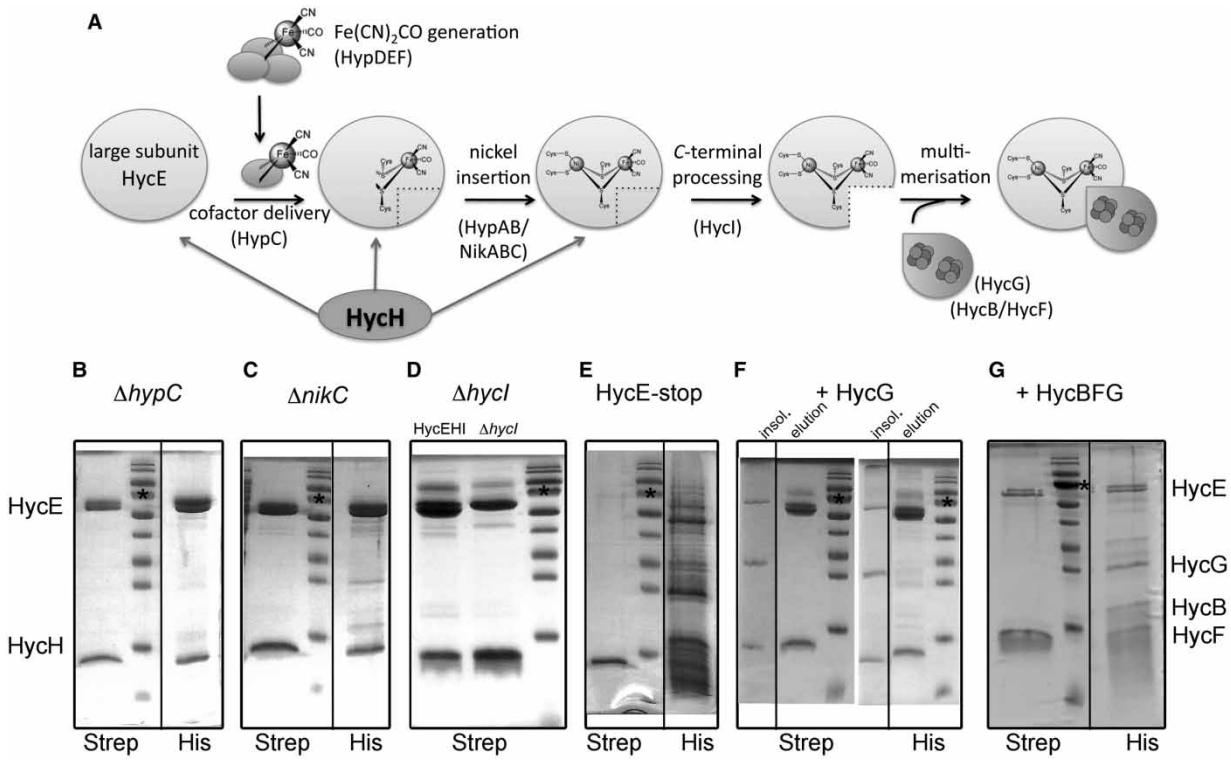

Figure 4. HycE and HycH interaction in maturation intermediates.

(**A**) The scheme summarises the maturation of HycE and the proteins involved. HycE is shown as an oval and initially receives the $Fe(CN)_2CO$ part of the [NiFe]-cofactor, which is synthesised by HypDEF and delivered by HypC. Subsequently, nickel is inserted by HypAB after being transported into the cell by NikABC. This step is the prerequisite for HycI-dependent proteolytic processing of HycE and further its interaction with the electron transfer subunits HybBFG (FeS clusters are indicated by small circles arranged as a cube). The unprocessed forms of HycE interact with HycH (arrows). Shown are purifications of pHycEHI in (**B**) CPH003 (Δ*hypC*), (**C**) CPH002 (Δ*nikC*), (**D**) pHycEH from CPH001, (**E**) pHycEstopHI from CPH001 and (**F**) pHycEHI from CPH001 in the presence of pHycG (+HycG) or (**G**) pHycBFG (+HycBFG) as indicated. The proteins were purified either by nickel (His) or Streptactin (Strep), as indicated below the gels. Every box shows a single gel, with the nickel and Strep purifications pasted next to each other from different lanes. The ladder is PageRuler prestained (Thermo Fisher) and the 70 kDa band has been marked with an asterisk.

The FHL complex is very similar to Complex I whose crystal structure has been resolved [31]. An FHL model based on that structure showed not only an interaction interface of HycE and HycG but also a predicted interaction between the C-terminal domain of HycF and HycE, whereby this domain wrapped around HycE [7]. Therefore, to test whether HycF might facilitate the interaction, plasmid pHycEHI was co-transformed with pHycBFG, which encodes all three iron–sulphur subunits of the FHL complex. After the purification of $_{Strep}$HycH, an interaction with HycE could be observed; however, when $_{His}$HycE was purified, a total of three proteins were attached to $_{His}$HycE (Figure 4G). Western blot analysis showed that the elution fraction contained HycG and also the Strep signal from HycH could be detected. The other protein at 21 kDa is possibly either HycB or more likely HycF (data not shown).

Mapping the interaction residues on HycH

To gain insights into which residues of HycH are involved in the HycE interaction, site-directed mutagenesis was used to construct 18 HycH variants in which 13 amino acid positions were exchanged. The chosen positions correspond to conserved residues based on an alignment of 1095 HycH proteins in the Uniprot database from various organisms (Supplementary Figure S3A). The nomenclature of the residues corresponds to the native HycH, although the mutations were introduced in the Strep-tagged variant. Initially, the mutated genes encoding these variants were transformed in the Δ*hycH* strain and the ability of the encoded proteins to restore FHL-dependent H_2 production was assessed using gas chromatography. Of these HycH variants, the Y30A,

Biochemical Journal (2017) **474** 2937–2950
DOI: 10.1042/BCJ20170431

Table 2 Complementation of Δ*hycH* strain with HycH variants

Variant HycH expressed in Δ*hycH* (JW2688KO)[1]	H_2 production (μmol H_2 $OD^{-1}_{600\ nm}$ ml culture^{-1})[2]	HycE presence after Strep purification	HycH presence after His purification
pHycH	9.5 ± 0.8	Not applicable	Not applicable
pY30A	3.4 ± 0.2	n.d.	No
pY31A	9.0 ± 0.5	Yes	Yes
pY30/31A	3.9 ± 0.1	n.d.	No
pH37N	3.3 ± 0.9	Yes	n.d.
pH37K	4.2 ± 0.6	Yes	n.d.
pH37A	5.3 ± 0.6	Yes	Yes
pH37/38A	5.3 ± 0.6	Yes	Yes
pH38A	8.6 ± 0.5	Yes	Yes
pC44A	8.7 ± 0.3	Yes	Yes
pC51A	8.8 ± 0.3	Yes	Yes
pR70/71A/K72A	9.3 ± 0.6	No	No
pR70A	7.8 ± 0.4	Yes	Yes
pR71A	8.3 ± 0.8	Yes	Yes
pK72A	11.0 ± 1.0	Yes	Yes
pY79A	8.1 ± 1.8	No	No
pE81A	9.0 ± 0.1	No	No
pH88A	8.4 ± 1.8	Yes	Yes
pY128A	6.8 ± 0.9	No	No

All measurements were done in biological triplicates and values are given as average with their respective standard deviations. Abbreviations: n.d., tagged protein was not detectable.
[1]Cells were grown anaerobically in 5 ml of TGYEP (pH 6.5) with a headspace of 10 ml.
[2]A volume of 200–500 μl of headspace was sampled for H_2 concentration and the amount of H_2 was calculated based on a calibration curve.

Y30/31A, H37N and the H37K variants were unable to complement the phenotype of Δ*hycH* deletion. The H37A, H37/38A and Y128A variants complemented only partially, while the individual exchanges of the above double mutant H38A and Y31A could complement to a similar level as the native protein. Of the other variants that were generated, all showed a similar ability to complement the mutant phenotype like the wild type (Table 2).

To screen the variants for their ability to interact with HycE, the plasmids were transformed into BL21(DE3) and the $_{Strep}$HycH variants or $_{His}$HycE were purified as described above. The results revealed that for the Y30A and Y30/31A variants, a protein corresponding in size to the expected mass of $_{Strep}$HycH appeared to aggregate as inclusion bodies and could neither be purified by Streptactin affinity chromatography nor was it detectable with the Streptactin-conjugate in Western blotting (data not shown). The $_{His}$HycE protein was purified without associated $_{Strep}$HycH variants Y30A and Y30/31A (Table 2 and Supplementary Figure S3). The Y31A single amino acid-exchange variant was not impaired in its ability to interact with HycE (Table 2 and Supplementary Figure S3). The interaction between $_{Strep}$HycH and $_{His}$HycE was also impaired in the Y128A exchange variant where both proteins could be purified only separately. The conserved residues H37, H38, C44, C51 and H88 had no influence on the interaction and they always co-purified HycE (Table 2).

Discussion

[NiFe]-hydrogenases can be classified according to their subunit composition, catalytic direction, membrane localisation and oxygen tolerance [32,33]. FHL belongs to the group 4(a) hydrogen-evolving hydrogenases that use formate as an electron donor and where energy conservation is unlikely [1]. Interestingly, while [NiFe]-hydrogenases are encoded in archaeal and bacterial genomes [32], no homologues of HycH are encoded in the operons of archaeal hydrogenases. For example, examination of the hydrogenase database HydDB

Biochemical Journal (2017) **474** 2937–2950
DOI: 10.1042/BCJ20170431

indicates that there are group 4a Hyd enzymes in the archaea species *Fervidicoccus fontis* and *Thermofilum pendens*, but these lack HycH [34]. The same applies for other group 4 hydrogenases like those from *Pyrococcus furiosus* (group 4d). According to the EggNOG database, the HycH protein can be found in firmicutes including *Moorella thermoacetica* and *Caldanaerobacter tengcongensis* and in all Proteobacteria except the Delta-clade [35]. All HycH proteins listed in the EggNOG database have a HycE subunit associated with them.

The initial characterisation of a Δ*hycH* strain concluded that it was impaired in large subunit processing and had no residual FHL activity which proved to be due to a polarity effect on the protease gene *hycI* [4]. The data shown here describe a Δ*hycH* phenotype for the first time and demonstrate that residual activity of FHL is detectable but that processing is not impaired. Thus, HycH is not essential for FHL activity; however, the activity is reduced by ∼90%. Nevertheless, FHL activity peaks at the same time during growth as the cells transition into stationary phase in Δ*hycH*, indicating that other aspects of maturation are not impaired. The instability of the FHL complex subunit HycG after 6 h is presumably due to faster protein turnover. While some activity is detectable in the early and late stationary phase, most of the HycG proteins are absent. The purification pattern follows this trend showing mainly the HycE catalytic subunit from the Δ*hycH* strain, but loss of the HycG and other attached proteins.

It appears that HyfJ partially contributes to the residual FHL activity in the *hycH* mutant background. As expected, the HyfG deletion of the Hyd-4 large subunit showed no contribution to total H_2 production under the tested conditions and confirms previous observations [29]. It has been stated that the synthesis of the Hyf proteins is not significant under the conditions employed here [11]. Nevertheless, the *hyfJ* gene is transcribed as has been observed before for other genes within the *hyf* operon [12] and apparently the influence of the *hyfJ* deletion indicates that Hyd-3 and Hyd-4 share components of their maturation machinery. Furthermore, the increased activities after complementation with HycH/HyfJ alone compared with those in the presence of extra copies of HycE/HyfG show that there is a competition of HycE and HyfG for the HycH and HyfJ proteins in the cell. This is substantiated by the partial interaction of HycE and HyfJ *in vitro* although part of the HycE protein is degraded, indicating a lack of the correct interaction partner. This also implies that HycH and HyfJ have a similar role in HycE and HyfG maturation, respectively. Future studies will be required to establish how the residual FHL activity in a strain lacking both HycH and HyfJ is generated.

The data shown here also indicate that HycH can only interact with the precursor form of HycE. These results also indicate that HypC is not required for the interaction of HycE and HycH although all three proteins were previously purified together [6]. Genetically processed HycE does not interact with HycH, and the addition of the small subunits HycF and HycG together could partially replace HycH. The small subunit HycG alone is not able to interact with HycE, presumably because it requires the shared interface with HycF for stability. However, we cannot currently explain the apparent double bands of the HycE protein under conditions where cofactor insertion is incomplete, e.g. in the Δ*nikC* and Δ*hypC* strains, and which, thus, should not result in HycI-dependent processing of HycE [36]. Both forms of HycE, however, also elute after the HycH Strep purification and only the lower band is visible when HycI is co-expressed. From the results obtained with the 'genetically processed' HycE, it can be deduced that processed HycE is not the correct interaction partner for HycH. There and also in the experiments with co-expressed HyfJ, a rapid degradation could hint to the lack of missing interaction partners. During purification of HycE alone, the protein tends to form precipitates (data not shown and [37]). The mixture of HycE after Strep purification could indicate dimer formation of processed and unprocessed HycE, where only the unprocessed HycE species interacts with HycH and mediates interaction with processed HycE. Unfortunately, based on the observed HycE double bands before metal insertion, no conclusion can be drawn about the specificity of the HycI processing in the employed expression system during later steps.

During the processing of HycE a 32 amino acid, C-terminal extension is removed making an arginine from the N-terminal side of the cleavage site the final residue [37,38]. In the processed HycE model structure, this Arg537 is buried within the protein, indicating a possible structural rearrangement after the proteolytic processing, as has been proposed for Hyd-2 [7,39]. The C-terminal extension of HycE itself has a total of 30% basic amino acids and HycH is predicted to be relatively acidic, however, with low conservation of these residues; thus, it is unlikely that the C-terminal extension is the interaction interface with HycH. Hence, the HycH protein might interact with residues that are not accessible after processing. Future work has to reveal the interface of HycE that interacts with HycH.

The predicted mature fold of HycE has a large basic interface with the small subunit HycG and two arginine residues of HycE (R218 and R239) co-ordinate the FeS cluster together with three cysteine residues from HycG

Biochemical Journal (2017) **474** 2937–2950
DOI: 10.1042/BCJ20170431

(Supplementary Figure S4A). Without the shared interface of HycE and HycG, the FeS cluster on HycG would be readily damaged or disassembled (Supplementary Figure S4B). Striking is the conservation of the Cys44, Cys51 and His residues at positions His37, His38 and His88 in HycH, respectively. These residues can generally be involved in FeS cluster binding [40]. The H37 residue in HycH is essential for the complementation of FHL activity, but surprisingly no difference for the interaction with HycE was observed with four independent exchanges. The extent to which the exchanges of H37 influence the activity of FHL varies, indicating that it is not a catalytic residue but rather an interacting amino acid. Therefore, one possible interaction partner other than HycE could be HycG for the protection of the FeS cluster by HycH, while the HycE subunit is loaded with the [NiFe]-cofactor. Evidence in favour of this hypothesis is presented by the data that show a more pronounced phenotype of the Δ*hycH* strain under conditions of iron depletion, whereby FeS insertion is impeded or delayed (Supplementary Table S1). Therefore, it is conceivable that HycH dissociates from HycE, allowing association with the small subunit triggering FHL assembly once the processing of HycE is completed. Hence, the requirement for HycH in slow-growing organisms, such as the archaea, could be dispensable, as they have enough time to assemble the complex independently of HycH or face other environmental conditions where metals are more abundant.

The residue Y128 of HycH that is involved in interaction with HycE has little direct influence on the specific activity of FHL. Furthermore, the combined mutations R70/71A/K72A, the Y79A and the E81A exchange interrupt the interaction with HycE. Therefore, the HycH variants can be classified into three main categories: first, the exchanges that have no influence on FHL activity or interaction with HycE; second and more interestingly, those that interrupt the interaction with HycE, but have no influence on FHL activity (R70/71/K72A, Y79A and E81A) and third, those that reduce FHL activity, but have unimpaired interaction with HycE (H37N, H37K). This function of HycH is reminiscent of the dual-function chaperones such as HupF from *Rhizobium leguminosarum* [41] and the HybE protein of *E. coli* Hyd-2, which interact with the precursor forms of both the large and small subunits [42].

In conclusion, the HycH protein is essential for efficient attachment and stability of the electron transfer subunit HycG and thus full activity of FHL. On the other hand, HycH interacts tightly with HycE and the residues involved in the interaction have no influence on FHL activity. Therefore, identification of further interaction partners will be the target of future studies.

Abbreviations

BV, benzyl viologen; FDH-H, formate dehydrogenase; FHL, formate hydrogenlyase; Hyd, hydrogenase; Hyd-3, [NiFe]-hydrogenase-3; Hyd-4, [NiFe]-hydrogenase 4; PAGE, polyacrylamide gel electrophoresis; RT–PCR, reverse transcription PCR.

Author Contribution

C.P. and F.S. designed the project and experiments. U.L., P.S., C.P. and J.S.M. performed the experiments. C.P. and F.S. wrote the manuscript.

Funding

This research was funded in Germany by the Deutsche Forschungsgemeinschaft [project PI 1252/2] and in the U.K. by the Biotechnology and Biological Sciences Research Council awards to F.S. [research grants BB/I02008X/1 and BB/L008521/1].

Acknowledgements

The authors thank Prof. R. Gary Sawers for discussions, support and reading the manuscript. Furthermore, Martin Herzberg is thanked for his support in metal analysis.

Competing Interests

The Authors declare that there are no competing interests associated with the manuscript.

References

1 Pinske, C. and Sargent, F. (2016) Exploring the directionality of *Escherichia coli* formate hydrogenlyase: a membrane-bound enzyme capable of fixing carbon dioxide to organic acid. *MicrobiologyOpen* **5**, 721–737 doi:10.1002/mbo3.365

2 McDowall, J.S., Murphy, B.J., Haumann, M., Palmer, T., Armstrong, F.A. and Sargent, F. (2014) Bacterial formate hydrogenlyase complex. *Proc. Natl Acad. Sci. U.S.A.* **111**, E3948–E3956 doi:10.1073/pnas.1407927111

3 Böhm, R., Sauter, M. and Böck, A. (1990) Nucleotide sequence and expression of an operon in *Escherichia coli* coding for formate hydrogenlyase components. *Mol. Microbiol.* **4**, 231–243 doi:10.1111/j.1365-2958.1990.tb00590.x
4 Sauter, M., Böhm, R. and Böck, A. (1992) Mutational analysis of the operon (*hyc*) determining hydrogenase 3 formation in *Escherichia coli*. *Mol. Microbiol.* **6**, 1523–1532 doi:10.1111/j.1365-2958.1992.tb00873.x
5 Rossmann, R., Maier, T., Lottspeich, F. and Bock, A. (1995) Characterisation of a protease from *Escherichia coli* involved in hydrogenase maturation. *Eur. J. Biochem.* **227**, 545–550 doi:10.1111/j.1432-1033.1995.tb20422.x
6 McDowall, J.S., Hjersing, M.C., Palmer, T. and Sargent, F. (2015) Dissection and engineering of the *Escherichia coli* formate hydrogenlyase complex. *FEBS Lett.* **589** (20PartB), 3141–3147 doi:10.1016/j.febslet.2015.08.043
7 Pinske, C. and Sawers, R.G. (2016) Anaerobic formate and hydrogen metabolism. *EcoSal. Plus* doi:10.1128/ecosalplus.ESP-0011-2016 PMID:27735784
8 Magalon, A. and Böck, A. (2000) Analysis of the HypC-HycE complex, a key intermediate in the assembly of the metal center of the *Escherichia coli* hydrogenase 3. *J. Biol. Chem.* **275**, 21114–21120 doi:10.1074/jbc.M000987200
9 Magalon, A. and Böck, A. (2000) Dissection of the maturation reactions of the [NiFe] hydrogenase 3 from *Escherichia coli* taking place after nickel incorporation. *FEBS Lett.* **473**, 254–258 doi:10.1016/S0014-5793(00)01542-8
10 Andrews, S.C., Berks, B.C., McClay, J., Ambler, A., Quail, M.A., Golby, P. et al. (1997) A 12-cistron *Escherichia coli* operon (*hyf*) encoding a putative proton-translocating formate hydrogenlyase system. *Microbiology* **143** (Pt 11), 3633–3647 doi:10.1099/00221287-143-11-3633
11 Self, W.T., Hasona, A. and Shanmugam, K. (2004) Expression and regulation of a silent operon, *hyf*, coding for hydrogenase 4 isoenzyme in *Escherichia coli*. *J. Bacteriol.* **186**, 580–587 doi:10.1128/JB.186.2.580-587.2004
12 Skibinski, D.A.G., Golby, P., Chang, Y.-S., Sargent, F., Hoffman, R., Harper, R. et al. (2002) Regulation of the hydrogenase-4 operon of *Escherichia coli* by the sigma(54)-dependent transcriptional activators FhlA and HyfR. *J. Bacteriol.* **184**, 6642–6653 doi:10.1128/JB.184.23.6642-6653.2002
13 Wu, L.-F., Mandrand-Berthelot, M.-A., Waugh, R., Edmonds, C.J., Holt, S.E. and Boxer, D.H. (1989) Nickel deficiency gives rise to the defective hydrogenase phenotype of *hydC* and *fnr* mutants in *Escherichia coli*. *Mol. Microbiol.* **3**, 1709–1718 doi:10.1111/j.1365-2958.1989.tb00156.x
14 Hamilton, C.M., Aldea, M., Washburn, B.K., Babitzke, P. and Kushner, S.R. (1989) New method for generating deletions and gene replacements in *Escherichia coli*. *J. Bacteriol.* **171**, 4617–4622 doi:10.1128/jb.171.9.4617-4622.1989
15 Baba, T., Ara, T., Hasegawa, M., Takai, Y., Okumura, Y., Baba, M. et al. (2006) Construction of *Escherichia coli* K-12 in-frame, single-gene knockout mutants: the Keio collection. *Mol. Syst. Biol.* **2**, 2006.0008 doi:10.1038/msb4100050
16 Miller, J. (1972) *Experiments in Molecular Genetics*, Cold Spring Harbor Laboratory, Cold Spring Harbor, NY
17 Cherepanov, P.P. and Wackernagel, W. (1995) Gene disruption in *Escherichia coli*: TcR and KmR cassettes with the option of Flp-catalyzed excision of the antibiotic-resistance determinant. *Gene* **158**, 9–14 doi:10.1016/0378-1119(95)00193-A
18 Pinske, C., Bönn, M., Krüger, S., Lindenstrauß, U. and Sawers, R.G. (2011) Metabolic deficiencies revealed in the biotechnologically important model bacterium *Escherichia coli* BL21(DE3). *PLoS ONE* **6**, e22830 doi:10.1371/journal.pone.0022830
19 Jacobi, A., Rossmann, R. and Böck, A. (1992) The *hyp* operon gene products are required for the maturation of catalytically active hydrogenase isoenzymes in *Escherichia coli*. *Arch. Microbiol.* **158**, 444–451 doi:10.1007/BF00276307
20 Begg, Y.A., Whyte, J.N. and Haddock, B.A. (1977) The identification of mutants of *Escherichia coli* deficient in formate dehydrogenase and nitrate reductase activities using dye indicator plates. *FEMS Microbiol. Lett.* **2**, 47–50 doi:10.1111/j.1574-6968.1977.tb00905.x
21 Sambrook, J. and Russell, D. (2001) *Molecular Cloning: A Laboratory Manual*. Cold Spring Harbor Laboratory, Cold Spring Harbor, NY
22 Hormann, K. and Andreesen, J.R. (1989) Reductive cleavage of sarcosine and betaine by *Eubacterium acidaminophilum* via enzyme systems different from glycine reductase. *Arch. Microbiol.* **153**, 50–59 doi:10.1007/BF00277541
23 Laemmli, U.K. (1970) Cleavage of structural proteins during the assembly of the head of bacteriophage T4. *Nature* **227**, 680–685 doi:10.1038/227680a0
24 Towbin, H., Staehelin, T. and Gordon, J. (1979) Electrophoretic transfer of proteins from polyacrylamide gels to nitrocellulose sheets: procedure and some applications. *Proc. Natl Acad. Sci. U.S.A.* **76**, 4350–4354 doi:10.1073/pnas.76.9.4350
25 Sargent, F., Stanley, N.R., Berks, B.C. and Palmer, T. (1999) Sec-independent protein translocation in *Escherichia coli*. A distinct and pivotal role for the TatB protein. *J. Biol. Chem.* **274**, 36073–36082 doi:10.1074/jbc.274.51.36073
26 Pinske, C. and Sawers, R.G. (2010) The role of the ferric-uptake regulator Fur and iron homeostasis in controlling levels of the [NiFe]-hydrogenases in *Escherichia coli*. *Int. J. Hydrogen Energy* **35**, 8938–8944 doi:10.1016/j.ijhydene.2010.06.030
27 Lowry, O., Rosebrough, N., Farr, A. and Randall, R. (1951) Protein measurement with the Folin phenol reagent. *J. Biol. Chem.* **193**, 265–275 PMID:14907713
28 Pinske, C., Krüger, S., Soboh, B., Ihling, C., Kuhns, M., Braussemann, M. et al. (2011) Efficient electron transfer from hydrogen to benzyl viologen by the [NiFe]-hydrogenases of *Escherichia coli* is dependent on the coexpression of the iron-sulfur cluster-containing small subunit. *Arch. Microbiol.* **193**, 893–903 doi:10.1007/s00203-011-0726-5
29 Redwood, M.D., Mikheenko, I.P., Sargent, F. and Macaskie, L.E. (2008) Dissecting the roles of *Escherichia coli* hydrogenases in biohydrogen production. *FEMS Microbiol. Lett.* **278**, 48–55 doi:10.1111/j.1574-6968.2007.00966.x
30 Wu, L.F. and Mandrand-Berthelot, M.-A. (1986) Genetic and physiological characterization of new *Escherichia coli* mutants impaired in hydrogenase activity. *Biochimie* **68**, 167–179 doi:10.1016/S0300-9084(86)81081-1
31 Efremov, R.G., Baradaran, R. and Sazanov, L.A. (2010) The architecture of respiratory complex I. *Nature* **465**, 441–445 doi:10.1038/nature09066
32 Peters, J.W., Schut, G.J., Boyd, E.S., Mulder, D.W., Shepard, E.M., Broderick, J.B. et al. (2015) [Fefe]- and [NiFe]-hydrogenase diversity, mechanism, and maturation. *Biochim. Biophys. Acta, – Mol. Cell Res.* **1853**, 1350–1369 doi:10.1016/j.bbamcr.2014.11.021
33 Vignais, P.M., Billoud, B. and Meyer, J. (2001) Classification and phylogeny of hydrogenases. *FEMS Microbiol. Rev.* **25**, 455–501 doi:10.1111/j.1574-6976.2001.tb00587.x
34 Søndergaard, D., Pedersen, C.N.S. and Greening, C. (2016) HydDB: a web tool for hydrogenase classification and analysis. *Sci. Rep.* **6**, 34212 doi:10.1038/srep34212
35 Huerta-Cepas, J., Szklarczyk, D., Forslund, K., Cook, H., Heller, D., Walter, M.C. et al. (2016) eggNOG 4.5: a hierarchical orthology framework with improved functional annotations for eukaryotic, prokaryotic and viral sequences. *Nucleic Acids Res.* **44** (D1), D286–D293 doi:10.1093/nar/gkv1248

Biochemical Journal (2017) **474** 2937–2950
DOI: 10.1042/BCJ20170431

36 Theodoratou, E., Paschos, A., Magalon, A., Fritsche, E., Huber, R. and Böck, A. (2000) Nickel serves as a substrate recognition motif for the endopeptidase involved in hydrogenase maturation. *Eur. J. Biochem.* **267**, 1995–1999 doi:10.1046/j.1432-1327.2000.01202.x
37 Rossmann, R., Sauter, M., Lottspeich, F. and Böck, A. (1994) Maturation of the large subunit (HYCE) of *Escherichia coli* hydrogenase 3 requires nickel incorporation followed by C-terminal processing at Arg537. *Eur. J. Biochem.* **220**, 377–384 doi:10.1111/j.1432-1033.1994.tb18634.x
38 Przybyla, A.E., Robbins, J., Menon, N. and Peck, H.D. (1992) Structure-function relationships among the nickel-containing hydrogenases. *FEMS Microbiol. Lett.* **88**, 109–136 doi:10.1111/j.1574-6968.1992.tb04960.x
39 Thomas, C., Muhr, E. and Sawers, R.G. (2015) Coordination of synthesis and assembly of a modular membrane-associated [NiFe]-hydrogenase is determined by cleavage of the C-terminal peptide. *J. Bacteriol.* **197**, 2989–2998 doi:10.1128/JB.00437-15
40 Imlay, J.A. (2006) Iron-sulphur clusters and the problem with oxygen. *Mol. Microbiol.* **59**, 1073–1082 doi:10.1111/j.1365-2958.2006.05028.x
41 Albareda, M., Manyani, H., Imperial, J., Brito, B., Ruiz-Argüeso, T., Böck, A. et al. (2012) Dual role of HupF in the biosynthesis of [NiFe] hydrogenase in *Rhizobium leguminosarum*. *BMC Microbiol.* **12**, 256 doi:10.1186/1471-2180-12-256
42 Dubini, A. and Sargent, F. (2003) Assembly of Tat-dependent [NiFe] hydrogenases: identification of precursor-binding accessory proteins. *FEBS Lett.* **549**, 141–146 doi:10.1016/S0014-5793(03)00802-0